LAWRENCE
LIVERMORE
NATIONAL
LABORATORY

UCRL-JRNL-234391

Shock-Compressed Diamond: Melt, Insulator-Conductor and Polymeric-Atomic Transitions

J. Eggert, D. G. Hicks, P. M. Celliers, D. K. Bradley, R. S. McWilliams, R. Jeanloz, J. E. Miller, T. R. Boehly

September 7, 2007

Nature Physics

Updated October 14, 2003

Shock-Compressed Diamond: Melt, Insulator-Conductor and Polymeric-Atomic Transitions

J. Eggert[1], D. G. Hicks[1], P. M. Celliers[1], D. K. Bradley[1], R. S., McWilliams[1,2], R. Jeanloz[2], J. E. Miller[3], T. R. Boehly[3], and G. W. Collins[1]

[1]Lawrence Livermore National Laboratory, Livermore, CA 94551
[2]University of California, Berkeley, CA 94720
[3]University of Rochester, Rochester, NY 14623

Temperatures measured on the shock-Hugoniot of diamond reveal melting between 650 (± 60) GPa and 9000 (± 800) K and 1090 (± 50) GPa and 8400 (± 800) K, with a heat of fusion of ~ 25 ±10 kJ/mole and a negative Clapeyron slope $\partial T/\partial P|_{melt}$ = – 5 ± 3 K/GPa. Thus, the fluid is denser than the compressed solid, and optical reflectivity measurements show it to be metallic. Hugoniot-temperature measurements extending to over 4000 GPa (40 Mbar) and 115,000 K suggest de-polymerization of a dense covalently-bonded fluid to an atomic state between 10,000 and 30,000 K. These experimental results indicate that carbon present deep inside planets such as Uranus and Neptune could be solid for through-going convection, whereas stable stratification would allow for the presence of fluid metallic carbon at depth; in either case, the presence of carbon could potentially affect planetary seismic normal modes.

Diamond, the hardest material known, has a high refractive index with large dispersion leading to its renowned 'fire', and very high Debye temperature and thermal conductivity. For these reasons diamond is not only a valued gemstone, but also a very important technological material. Below 1.5 GPa, diamond is the prototypical meta-stable phase having an extremely long lifetime at standard temperature (*T*) and pressure (*P*), but it converts to graphite within seconds above 2100 K(*1*) and melts to liquid carbon at about 4600 K(*2, 3*).

Carbon is the fourth most-abundant element in the solar system. Since Ross proposed "diamonds in the sky" in 1981,(*4*) the idea of significant quantities of pure carbon existing in giant planets such as Uranus and Neptune has gained both experimental(*5*) and theoretical(*6*) support. It is now accepted that the high-*P*, high-*T* behavior of carbon is essential to the modeling of planetary interiors.(*7*)

No direct temperature measurements of the diamond-melt curve have ever been reported. However there are many theoretical studies of high-pressure melting.(*8-12*) These studies suggest that the fluid is conducting, the coordination number increases beyond 4, and the melt curve reaches a maximum temperature before decreasing with pressure. Due to the high pressures and temperatures involved, experimental attempts to measure the diamond melt curve have proven difficult.(*13*) By extrapolating the intersection of the graphite/diamond and the graphite/liquid phase lines the triple point between graphite, diamond and liquid was estimated to be 4400 K and 14 GPa.(*2, 3, 14, 15*) Static experiments show the diamond melt curve has a positive Clapeyron slope, $\partial T/\partial P|_{melt} > 0$ up to 60 GPa. (*13, 16-18*) This is significant because the Clapeyron equation, $\partial T/\partial P|_{melt} = \Delta V_m/\Delta S_m|_{P,T}$, where ΔV_m and ΔS_m are the volume and entropy changes on the melt line, relates the slope to the sign of the density change $\Delta\rho_m$ since $\Delta S_m > 0$.

Strong shocks are a powerful tool for studying high-pressure phase transitions, equation of state, and other material properties. The shock Hugoniot is the locus of all final states of *P*, energy (*E*), density (ρ), shock velocity (*Us*), and particle velocity (*Up*) that are achieved in a material behind a single shock wave traversing a given initial state. These quantities are related by three Hugoniot relations(*19*), but temperature and electrical conductivity are not part of the Hugoniot relations and must be measured independently.

From shock experiments on graphite it has been inferred that diamond remains solid up to 143 GPa and 6500 K, and the diamond melt curve has $\partial T/\partial P|_{melt} > 0$ up to at least 300 GPa. (*20-22*) The diamond Hugoniot has recently been measured up to about 4000 GPa.(*23-25*) There is evidence of a shift in the Hugoniot at around 750 GPa that suggests melting with a negative Clapeyron slope, however this result is subtle and not a robust signature of melt. (*24, 25*) Optical reflectivity measurements showed that shock-compressed diamond continuously increases in electrical conductivity between 600 and 1000 GPa. It was found that the reflectivity was best fit by assuming a continuously-increasing conducting-fluid fraction as the shock traversed the coexistence region.(*26, 27*)

Following Hicks et al.,(*28*) we studied shock states over a large pressure region of the diamond Hugoniot using a monotonically-decaying shock propagating in diamond. Targets consisted of ~500 μm-thick diamond disks glued to a 50 μm-thick aluminum disk as shown in figure 1A.(*27*) The OMEGA laser (1 ns drive pulse) produced

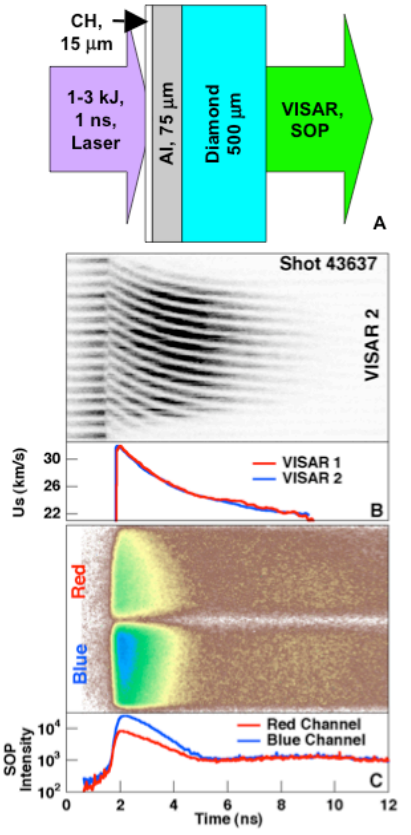

Figure 1. A) Sketch of diamond melt target. B) VISAR record for polycrystalline diamond experiment and analyzed velocity data. C) Two-color pyrometer data together with line-outs for each color (Blue = 450 nm, Red = 650 nm).

strong unsupported shocks that decayed as they transited the sample to ~ 30% of the maximum pressure.(*27*) The decaying-shock front continually encountered new, un-shocked material as it propagated, and thus is treated as having initiated a continuum of 'single-shock' experiments at successively lower pressures. For most of the decay, the shock front was reflecting and the instantaneous shock velocity (*Us*) and shock-front reflectance (*R*) at 532 nm was measured using a velocity interferometer (VISAR). (*27*) Typical VISAR data and shock-velocity history are shown in figure 1B.

At the same time, the absolute spectral radiance of the shock, $I(\lambda)$ centered at two wavelengths (650 and 450 nm) was measured using a streaked optical pyrometer (SOP). $I(\lambda)$ combined with the reflectivity determined from the VISAR traces were used to determine the shock temperature. (*27*) A streaked image of the thermal emission together with a lineout from each SOP wavelength is shown in figure 1C. From this image, it is evident that the thermal emission rises quickly when the shock enters the diamond at ~1.8 ns (~32 km/s), then decays along with the shock velocity between ~2 and 6 ns (~32 and ~24 km/s). However, between 6 and 10 ns (24 and < 22 km/s), as the shock velocity (pressure) continues to decrease, the thermal emission increases slightly (not visible at the scale of Fig. 1C). This increase in emission was observed in every experiment at very reproducible shock velocities and, as described below, is interpreted as the onset of a fluid-solid coexistence region.

Figure 2 shows the resulting *T* versus measured *Us* for nine experiments: four natural single-crystal (type 1a, [110]-oriented) and five CVD micro-crystalline diamond samples. The black curve is the weighted mean and the error bars denote the weighted standard deviation of the nine experiments. As is evident from the raw-data for a decaying shock (Fig. 1), *T* decreases with decreasing *Us* from 42 to 24 km/s and then begins to increase. This dramatic change in *T* vs *Us* is interpreted as the transition from the pure-fluid phase ($Us \gtrsim 24$ km/s) to the mixed-phase region where solid and fluid phases coexist ($Us \lesssim 24$ km/s). Figure 2A shows shock reflectivity versus *Us* for the same set of experiments. At the highest

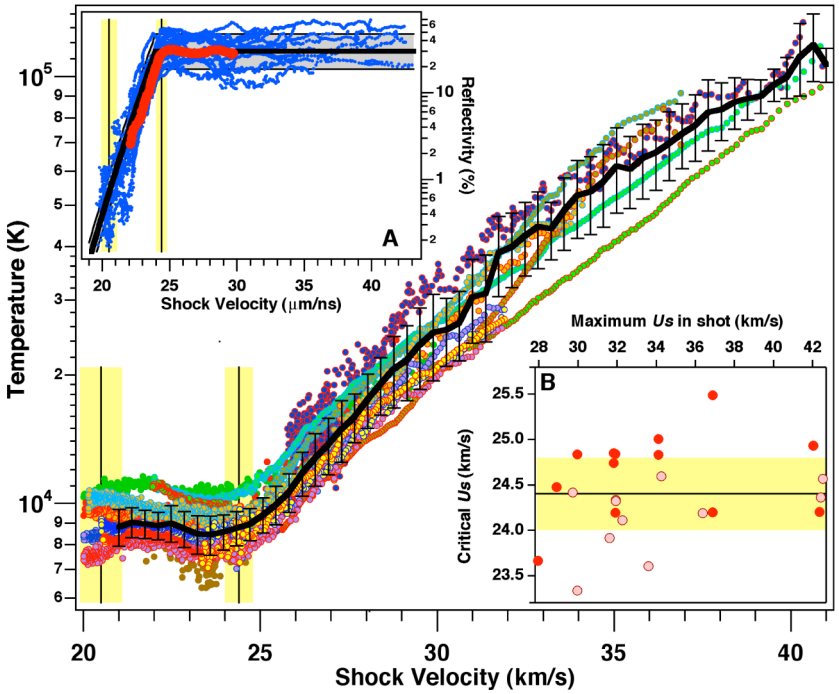

Figure 2. Temperature vs shock velocity for all the data collected (nine separate experiments were performed, but the two VISARs and two SOP wavelengths were treated separately so that more than nine data sets are plotted in this figure). A) Shock reflectance for our data (blue) together with an earlier result from Bradley, et al. (red). The black line was used for determining the emissivity and its uncertainty in determining the temperature. B) The fitted trace-by-trace determination of *T-Us* kinks (red) and reflectivity plateau (pink) used to find the upper range of the mixed-phase region. The mean and standard deviation of these independent determinations and the reflectivity at 0.5% are shown by the shaded lines in Figs. 2 and 3.

Us, the optical properties of carbon show that it is electrically conducting with $R \approx 30\%$. At $Us \lesssim 24$ km/s, the reflectivity decreases monotonically to the detection limit of $\sim 0.5\%$.

If the melt transition is fast and the shock front is in equilibrium, then the measured *P*, *T* path follows the melt curve within the mixed-phase region. Alternatively, it is possible that melting occurs suddenly from a superheated solid to a pure fluid with no mixed-phase region.(*29*) In the case of diamond, two factors suggest that the melt line is followed through a mixed-phase region and superheating is not a factor. First, there is no rapid change in temperature over a small pressure range as is observed for superheating.(*29*) It should be noted that the same technique used here previously documented a rapid temperature change consistent with superheating for both quartz and fused silica.(*28*) Second, the reflectivity increases smoothly between 650 and 1090 GPa. It was found previously that simple modeling of this reflectivity increase required a conducting-fluid phase with a continuously increasing volume fraction.(*26, 27*) These observations support the hypothesis of quasi-equilibrium melting along a coexistance curve rather than a superheated solid followed by discontinuous melting (which would imply sudden jumps in both the temperature and reflectivity).

In order to accurately locate the transition from mixed-phase to pure-fluid, both *T* vs. *Us* and *R* vs. *Us* were fitted by power laws joined continuously at an adjustable critical shock velocity Us^{crit}. The Us^{crit} from each of the fits is shown in figure 2B, with the weighted means and standard deviations being $Us^{crit} = 24.6 \pm 0.4$ and 24.3 ± 0.3 km/s for the fits to *T* and the *R* respectively. This agreement for Us^{crit} determined by two independent observations reinforces the conclusion that diamond melts completely to a metallic fluid at 24.4 ± 0.4 km/s (1090 ± 50 GPa) and 8400 ± 800 K.

A comparable kink in *T* vs. *Us* could not be observed at the pure solid to mixed-phase transition. First, since the

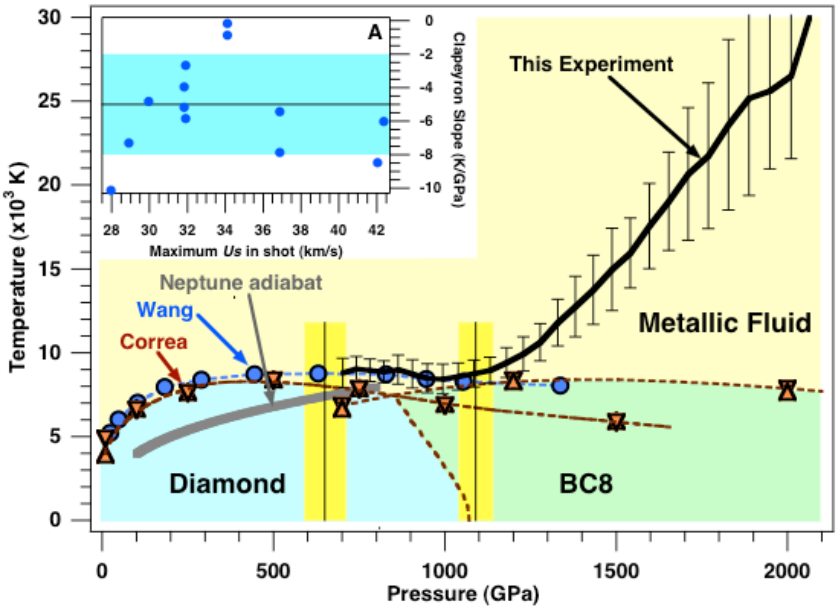

Figure 3) Temperature vs pressure data (black line with error bars) together with density functional theory from Wang, Scandolo, and Car (blue circles) which include diamond and the liquid phase, and Correa, Bonev, and Galli (brown triangles) which include the diamond, BC8, and fluid phases. The graphite phase was omitted for clarity. A) Clapeyron slope determined for each individual shot by fitting the temperature between 810 and 980 GPa to a line. Note that every shot has a negative slope and the average Clapeyron slope is -5±3 K/GPa.

solid phase is not reflecting, *Us* was not measured directly. Second, the thermal emission from the non-reflecting solid (large absorption depth) was not necessarily confined to the shock front, and was likely dominated by the higher-temperature material behind the shock front.(*27*) For this reason, the onset of melting was identified simply by the onset of reflectivity. The average shock velocity for reflectivity of 0.5% is $Us^{R=0.5\%} = 20.5 \pm 0.6$ km (650 ± 60 GPa) and 9000 ± 800 K.

Each individual shot clearly showed a negative Clapeyron slope $\partial T/\partial P|_{melt}$ in the mixed-phase region, To illustrate this, the inset to figure 3 shows the fitted Clapeyron slope for each shot. The weighted-mean Clapeyron slope is $\partial T/\partial P|_{melt} = -5 \pm 3$ K/GPa . (All conversions from *Us* measurements to pressure in this report use the previously-measured shock Hugoniot for the fluid phase, $Us = C + sUp$, where $C = 10.99$ km/s and $s = 1.052$,(*24*) and $P(Us) = \rho_0 Us(Us - C)/s$, which follows from the Rankine-Hugoniot relations.)

Figure 3 compares the weighted-mean *T* vs. *P* with recent first-principles molecular-dynamics (MD) calculations of the melt curve.(*11, 12*) Impressively, the simulations and experimental melt curves agree closely. As observed experimentally, the simulations predicted a conducting fluid and a negative Clapeyron slope above 500 GPa, attributed to a continuously-increasing liquid coordination number.(*11, 12*)

A high-pressure BC8 solid phase has often been proposed by analogy with silicon and germanium(*30*) and by total-energy calculations(*9, 12*). This phase was included in one of the MD simulations(*12*) which predicted that the diamond Hugoniot (not shown) may cross the diamond-BC8-liquid triple point. The new data presented here do not distinguish which phase is melting (diamond or BC8) and are not sensitive enough to probe the existence of a triple point.

Further analysis suggests that melting does not represent the only structural changes revealed by the present data for carbon. The high specific heat, C_V , in the fluid phase shows that carbon likely undergoes extensive structural change with a reconfiguration energy much larger than the latent heat of melting.

Following the analysis introduced by Hicks et al.,(*28*) the specific heat is given by:

$$C_V = \frac{\Delta E_V}{\Delta T_V} = \frac{\Delta E_H - \Delta E_S}{\Delta T_H - \Delta T_S} = \frac{\partial E/\partial V|_H + P}{\partial T/\partial V|_H + \Gamma T/V}$$

where Γ is the Gruneisen parameter, and the subscript *H* identifies a change along the Hugoniot, *S* along an isentrope, and *V* along an isochore. The experimental fit for *Us*, *Up* by Bradley et al.(*24*) used above determines *E*, *V*, and *P*. *T* was measured here, so that the only parameter in the equation that has not been directly measured is Γ . Johnson showed that for strong shocks where significant shock heating occurs $\Gamma \approx 2(s-1)$.(*31*) Since $s = 1.05$ for strongly-shocked diamond(*24*) the Gruneisen parameter is expected to be very small, $\Gamma \approx 0.10$. Even so, C_V is quite insensitive to the value of Γ since $\partial T/\partial V|_H$ exceeds T/V by a factor of 3 to 6. In other words, for fluid carbon the *T* rise along the Hugoniot is large compared to the *T* rise along the isentrope.

Figure 4 shows the results of this calculation of C_V . The broad peak in C_V of $\sim 4Nk_B$ between 10,000 and 30,000 K is strikingly similar to that previously reported for quartz and fused silica(*28*), and likely has a similar interpretation: a reconfiguration of atomic packing after melt. Note that the optical reflectivity is constant over this *T-P* range, so that it is unlikely that a change

in the ionization fraction contributes significantly to the peak in the heat capacity. Following Hicks et al.(*28*) the excess specific heat (defined as that

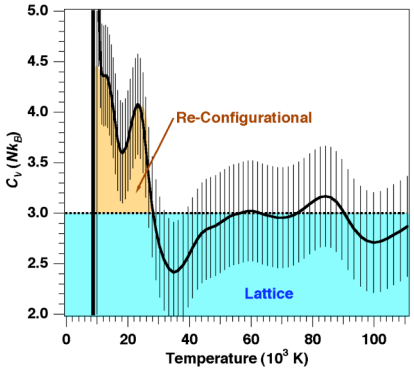

Figure 4. Specific heat vs. temperature showing the lattice component, and the peak attributed to atomic-bonding reconfiguration after melt. Note that at the temperatures and pressures where this peak in the heat capacity exists the phase is pure liquid and the reflectivity is constant.

exceeding the Dulong-Petit value of $3Nk_B$) was integrated to get a re-configurational energy of 200±50 kJ/mol (2.1±0.5 eV/atom). This corresponds to the difference in binding energy between the polymeric, covalently-bonded fluid near melting, and the high-temperature monatomic fluid. For comparison, the enthalpy of formation for diamond is $\simeq 720\ \mathrm{kJ/mol}$ (7.5 eV/atom), and the (largely compressional) energy difference on melting along the Hugoniot can be found from the Rankine-Hugoniot relations to be, $\Delta E_m = 430 \pm 70$ kJ/mole. The latent heat of melting can be estimated by considering disorder- and volumetric- entropy changes, combined with the Clapeyron relation as (*27*)

$$L = T\Delta S_m \approx TR\ln 2 \Big/ \left(1 - \frac{\Gamma c_V}{V}\frac{\partial T}{\partial P}\Big|_{melt}\right).$$

The latent heat estimated in this way, $L \approx 25 \pm 10$ kJ/mole, is much smaller than the re-configurational energy estimated above, which includes effects of finite compression along the Hugoniot. The relative density change at melt can likewise be estimated as, $\Delta\rho/\rho = -\rho\Delta S_m \partial T/\partial P|_{melt} \approx 2 \pm 1\%$. This is roughly consistent with estimates based on recent Hugoniot experiments which yield $\Delta\rho/\rho$ ranging from 2-4%(*24*) to 5-14%(*25*), and MD simulations that give ~1%(*11*).

Finally, we consider the implications of the measured melt curve to giant-planet interiors. Figure 3 includes a proposed adiabat for Neptune's interior temperature distribution assuming through-going convective mixing. (*7, 32*) Given this model and the melt curve, pure carbon within giant planets (*4-6*) would be solid at all depths. However, it is possible that a hotter deep interior may exist, dynamically isolated from the outermost atmosphere by a stably-stratified, non-convecting region within Uranus and Neptune.(*7, 32, 33*) In such warmer conditions, pure carbon could exist in the liquid metallic state, settling out of the mantle to form an outer core sustaining the planetary magnetic field above a denser rocky inner core. In either case, the high sound velocity of a carbon layer at depth could influence planetary normal modes that may be observable in the future.

Acknowledgements: We thank Walter Unites for his support in preparing the diamond samples. This work was performed under the auspices of the U.S. Department of Energy by University of California, Lawrence Livermore National Laboratory under Contract W-7405-Eng-48.

References and Notes

1. V. R. Howes, *Proc. Phys. Soc.* **80**, 648 (1962).
2. F. P. Bundy, *J. Chem. Phys.* **38**, 618 (1963).
3. M. Togaya, S. Sugiyama, E. Mizuhara, in *High Pressure Science and Technology* S. C. Schmidt, J. W. Shaner, G. A. Samara, M. Ross), Eds. (AIP Conference Proceedings, Colorado Springs, CO, 1993), vol. 309, pp. 255.
4. M. Ross, *Nature* **292**, 435 (1981).
5. L. R. Benedetti *et al.*, *Science* **286**, 100 (1999).
6. F. Ancilotto, G. L. Chiarotti, S. Scandolo, E. Tosatti, *Science* **275**, 1288 (1997).
7. T. Guillot, *Annu. Rev. Earth Planet. Sci.* **33**, 493 (2005).
8. G. Galli, R. M. Martin, R. Car, M. Parrinello, *Science* **250**, 1547 (1990).
9. M. P. Grumbach, R. M. Martin, *Phys. Rev. B.* **54**, 15730 (1996).
10. C. J. Wu, J. N. Glosli, G. Galli, F. H. Ree, *Phys. Rev. Lett.* **89**, 135701 (2002).
11. X.-f. Wang, S. Scandolo, R. Car, *Phys. Rev. Lett.* **95**, 185701 (2005).
12. A. A. Correa, S. A. Bonev, G. Galli, *Proc. Nat. Acad. Sci.* **103**, 1204 (2006).
13. F. P. Bundy *et al.*, *Carbon* **34**, 141 (1996).
14. F. P. Bundy, *J. Chem. Phys.* **38**, 631 (1963).
15. N. S. Fateeva, L. F. Vereshchagin, *JETP Lett.* **13**, 110 (1971).
16. J. S. Gold, W. A. Bassett, M. S. Weathers, J. M. Bird, *Science* **225**, 921 (1984).
17. M. S. Weathers, W. A. Bassett, *Phys. Chem. Minerals* **15**, 105 (1987).
18. M. Togaya, in *Science and Technology of New Diamond* S. Saitro, O. Fukunaga, M. Yoshikawa, Eds. (KTK Scientific Publishers, Tokyo, Japan, 1990) pp. 369-373.
19. Y. B. Zel'dovich, Y. P. Raizer, *Physics of Shock Waves and High Temperature Hydrodynamic Phenomena* (Academic Press, New York, 1966), pp.
20. W. H. Gust, *Phys. Rev. B* **22**, 4744 (1980).
21. F. W. Shaner, J. M. Brown, C. A. Swenson, R. G. McQueen, *J. Phys. (Paris), Colloq.* **45**, c8 (1984).
22. L. E. Fried, W. M. Howard, *Phys. Rev. B.* **61**, 8734 (2000).
23. H. Nagao *et al.*, *Phys. Plasmas* **13**, 052705 (2006).
24. D. K. Bradley, P. M. Celliers, J. H. Eggert, D. G. Hicks, G. W. Collins, *J. Appl. Phys.*, submitted (2006).
25. S. Brygoo *et al.*, *Nature Materials* **6**, 274 (2007).
26. D. K. Bradley *et al.*, *Phys. Rev. Lett.* **93**, 195506 (2004).
27. *Information on materials and methods is available on Science Online.*
28. D. G. Hicks *et al.*, *Phys. Rev. Lett.* **97**, 025502 (2006).
29. S.-N. Luo, T. J. Ahrens, *Physics of Earth and Planetary Interiors* **143–144**, 369 (2004).
30. R. Biswas, R. M. Martin, R. J. Needs, O. H. Nielsen, *Phys. Rev. B* **35**, 9559 (1987).
31. J. D. Johnson, in *Shock Compression of Condensed Materials* S. C. Schmidt, Ed. (AIP, New York, 1998), vol. AIP Conf. Proc. No. 429, pp. 27.
32. W. B. Hubbard, M. Podolak, D. J. Stevenson, in *Neptune and Triton.* (University of Arizona Press, Tucson, AZ, 1995) pp. 109.
33. S. Stanley, J. Bloxham, *Nature* **428**, 151 (2004).